

Infrared high angular resolution measurements of stellar sources^{*}

III. Angular diameters and effective temperatures of eleven late-type giants

A. Richichi¹, S. Ragland¹, and L. Fabbioni²

¹ Osservatorio Astrofisico di Arcetri, Largo Enrico Fermi, 5, I-50125 Firenze, Italy

² Dipartimento di Statistica, Viale Morgagni 59, I-50134 Firenze, Italy

Received 5 August 1997 / Accepted 25 August 1997

Abstract. Near-infrared lunar occultation observations of eleven late-type giants in the spectral range K0 to M6 (including one carbon star) are reported here. These stars are resolved from our observations carried out at $2.2\mu\text{m}$, resulting in accurate determinations of their angular sizes, with values in the range 1.4 to 7.1 milliseconds of arc (mas) and a typical accuracy of 0.12 mas. Nine out of eleven sources are resolved for the first time.

In addition, near infrared photometric observations of some of the sources have been carried out to compute stellar bolometric fluxes, and hence derive the effective temperatures. Our accurate angular diameter measurements (at least in the case of eight sources) have the potential to provide effective temperatures with an accuracy less than 3% when bolometric fluxes become available with an accuracy less than 10%. The observed sources are discussed in conjunction with earlier high angular resolution observations and available photometric data. A comparison of the current performance of lunar occultations and long baseline interferometry in the field of angular diameters and effective temperatures is presented.

Key words: occultation – stars: fundamental parameters – stars: late-type – stars: circumstellar matter

1. Introduction

The importance of angular diameter measurements is related mainly to the fact that this is the only means to determine directly the effective temperature of a star, independently from its distance and any model-dependent assumptions. The effective temperature in turn is one of the fundamental parameters

needed to compare theories of model atmospheres against observation, and its calibration is still uncertain especially for the coolest spectral types. Another aspect is that, by means of the Hipparcos parallaxes, it is becoming possible to convert angular to linear diameters for an increasingly larger number of stars, thus providing direct checks for current theoretical models.

We will not discuss in detail in this paper these themes, as they will be the subject of a separate, more general work to be presented elsewhere. However, this is sufficient to motivate our ongoing effort to measure angular diameters, especially for the coolest stars. Some results have been published already by our group in this area, the most recent ones being described in Richichi et al. (1995) and Ragland et al. (1997). In particular, in this paper we will describe our measurement of the angular diameter for eleven late-type giants in the spectral range K0 to M6, including one carbon star. We will also present photometric data, necessary to compute the bolometric flux which has been used, together with the angular diameter, to derive the effective temperatures. Similar material has been presented already in Richichi et al. (1992a, 1992b; Papers I and II respectively hereafter). Since it is likely that such results will continue in the near future, we have decided to adopt from now on a common title, and number the papers in their subtitles; accordingly, this is then Paper III in this series. The material will be described and organized following the style of Paper II.

The technique used to obtain the angular diameters described in this paper is that of lunar occultations (LO). Traditionally, this technique has been the most productive in this area, with 127 stars (many of which with independent repeated measurements) listed already in the compilation of White & Feigman (1987). Since then, several more have been added (Richichi 1997). In spite of several disadvantages, LO continue to be a competitive and productive technique thanks to their simplicity and to the fact that they permit the achievement of resolution at the level of one milli-arcsecond (mas) even to small and medium sized telescopes. At the same time, one should recognize that more modern techniques such as long-baseline interferometry (LBI) are becoming steadily more reliable and readily available, making a major contribution in the area of angular

Send offprint requests to: A. Richichi (arichichi@arcetri.astro.it)

^{*} Based on observations collected at TIRGO (Gornergrat, Switzerland), at Calar Alto (Spain), and at the European Southern Observatory (La Silla, Chile). TIRGO is operated by CNR-CAISMI Arcetri, Italy. Calar Alto is operated by the German-Spanish Astronomical Center.

Table 1. Summary of the occultation observations

(1) Source	(2) Date UT	(3) Event	(4) Tel.	(5) PA °	(6) D "	(7) Δt ms	(8) τ ms	(9) Notes
SW Gem	23-09-89	R	C3	289	6	1.39	–	IR excess
AX Gem	07-01-93	D	C3	134	6	1.86	–	IR excess
IRC+20133	03-02-93	D	T	41	28	2.74	2.40	
T Ari	24-12-93	D	C1	52	21	2.00	–	IR excess
IRC–20307	18-07-94	D	C2	120	17	2.00	–	IR excess
IRC–20445	20-07-94	D	C2	130	17	2.00	–	previous angular diameter by LO; IR excess
IRC–20550	22-07-94	D	C2	144	17	2.00	–	LO binary; previous angular diameter by LO
AB Gem	28-09-94	R	T	335	28	3.43	3.01	IR excess
IRC+20071	15-09-95	R	T	255	28	2.42	2.00	LO binary
IRC+10034	11-10-95	R	T	276	28	5.42	5.00	
IRC+20141	15-10-95	R	T	352	21	2.42	2.00	LO binary

diameters. Recent results include those of Dyck et al. (1996) and Perrin et al. (1997). Typically, LBI and LO measurements have operated in different resolution ranges, the former having a median of the resolved angular diameters close to 15 mas (Perrin et al. 1997), and the latter close to 5 mas (Richichi 1997). However, this gap will soon vanish as longer baselines and more sensitive instruments will come into LBI facilities. This highlights an important role of LO measurements, namely to provide an independent means of checking the high angular resolution results of improved LBI observations.

2. Observations and data analysis

The observational details of the recorded events reported in this paper are summarized in Table 1, in a format very similar to that used in previous papers (see for instance Richichi et al. 1996b). In column (1) and (2) we list the source name and the date of the event. Column (3) lists the symbols denoting the event type, D for disappearance and R for reappearance. Column (4) lists the symbols to identify the telescope used: T denotes the 1.5 m TIRGO telescope, while C1, C2 & C3 denote the Calar Alto 1.23, 2.2 & 3.5 m telescopes respectively. In column (5) through (8) we list the predicted position angle of occultation, the aperture of the photometer, the sampling time of the lightcurve and the integration time of each data point. The last column is used for remarks, that are explained in more detail in Sect. 3. Table 2 lists cross-identifications of the observed sources in various catalogues, as well as some source details.

All occultations were observed with fast photometers, the characteristics of which as well as of the filters used are described in Richichi et al. (1996b), and references therein. All events reported here were night time events except the occultation of IRC+20071 which was recorded at twilight.

The LO observations were complemented when possible by near-infrared photometry in the JHKLM bands, which is reported in Table 3. This was carried out with the 1.5m telescope at TIRGO, 1.23m telescope at Calar Alto and 2.2m telescope at ESO (this latter denoted as E in the table). Note that the K

magnitudes listed in Table 2 are taken from the literature, and there can be some difference with our determinations due most likely to intrinsic variability of the source. In the computation of the bolometric fluxes (see Sect. 3.8), the values listed in Table 3 were preferred, since they were taken close to the date of occultation whenever possible. Also at TIRGO, the LONGSP spectrometer (Gennari & Vanzi 1994) was employed to obtain a near-IR spectrum of AB Gem (see Sect. 3.5).

The observed occultation lightcurves were analysed using a standard nonlinear least squares method to recover the high angular resolution information present in the data. Our data reduction program is based on the scheme originally proposed by Nather & McCants (1970), but incorporates important additions, such as the provision to account for the effects of scintillation, the finite time response of the instrument and spurious frequencies (generally due to mains pickup, or to telescope oscillations excited by wind), if any. The data reduction procedure has been discussed in more detail in Paper I.

3. Results and discussion

The stellar angular diameters derived from our LO data are listed in Table 4. Instead of showing all the lightcurves and the corresponding fits, we show in Fig. 1 only some cases, selected to illustrate different situations of angular diameter, atmospheric scintillation, telescope aperture and filter bandwidth. Some of the sources in our sample do not have sufficient earlier observations to discuss them at present. The other sources are discussed below briefly.

3.1. SW Gem

The occultation lightcurve of SW Gem is shown in Fig. 1a, from which it can be seen that scintillation corrections are essential to obtain an accurate estimation of the angular diameter. A polynomial of degree 4 with 3 free parameters has been used to account for the scintillation effect. This star is a semi-regular variable of period $P=680^d$ and amplitude of variability $\Delta V \sim 1.4$ mag

Table 2. Cross identifications of the occulted sources and their characteristics

Source	TMSS	IRAS	SAO	HD	Other	V	K	Sp.
SW Gem	+30170	06564+2606		267341	BD+26 1412	8.9	1.88	M5 III Var
AX Gem	+20153	06341+2109		260525	RAFGL 970	9.0	1.69	M5
IRC+20133	+20133	06065+2211	78045	42049	HR 2169	5.93	2.08	K4 III
T Ari	+20049	02455+1718	93115	17446	AFGL 379	7.3	0.3	M6
IRC−20307	−20307	16039−2040					2.53	M6
IRC−20445	−20445	18093−2107					1.94	M1 / M4
IRC−20550	−20550	19147−1902	162413	180540	43 Sgr	4.96	2.20	K0 III
AB Gem	+20145	06232+1906		45087	AFGL 937	> 8.2	2.55	N Var
IRC+20071	+20071	04051+1712	93777	26038	HR 1280	5.89	2.32	K5 III
IRC+10034	+10034	02541+1424	93196	18310	AFGL 404	8.8	1.3	M4
IRC+20141	+20141	06127+1818	95456	43185	BD+18 1141	6.61	2.87	K2 III

Table 3. Near infrared photometry

Source	Date	Tel.	J	H	K	L	M
SW Gem	06-11-92	T	3.24±0.01	2.19±0.02	1.98±0.02	1.67±0.04	
AX Gem	28-09-93	C1	3.06±0.05	2.08±0.03	1.77±0.03		
IRC+20133	28-09-93	C1	3.16±0.05	2.30±0.03	2.12±0.03		
T Ari	25-10-94	C1	1.83±0.05	1.18±0.39	0.48±0.05		
IRC−20550	17-07-95	E	3.31±0.08	2.79±0.09	2.71±0.05	2.62±0.02	2.71±0.10
AB Gem	23-10-94	T	4.94±0.02	3.58±0.02	2.66±0.02	1.89±0.03	
AB Gem	25-10-94	T	4.90±0.02	3.57±0.01	2.70±0.01	1.98±0.02	

(Kukarkin et al. 1958). The spectral type is M5 III (Bidelman 1980).

The IRAS LRS spectrum of this source shows a silicate feature in emission at $10\mu\text{m}$ (Olson et al. 1986). A radiative model fit to the IRAS colors and the silicate feature strength has been carried out by Hashimoto (1994) for a sample of oxygen rich AGB stars and the dust shell parameters have been derived. The reported value for the inner dust shell radius was $20 R_*$ at a temperature of 663 K, while the outer shell radius was $316 R_*$. There is no signature of circumstellar dust in our occultation data, as explained in Sect. 3.8. SW Gem was not detected in the search for OH (Chengalur et al. 1993) and H_2O (Lewis 1992; Dickinson 1976) emissions.

3.2. T Ari

The occultation lightcurve of T Ari is shown in Fig. 1b. The data have been affected by scintillation noise of relatively higher frequencies in the range 20-30 Hz, while at lower frequencies some signatures of the oscillating frequency of the telescope structure subject to strong wind could be seen. A polynomial of degree 7 with 6 free parameters has been adopted, and 3 more monochromatic frequencies have been removed. T Ari is a semi-regular variable of period 323^{d} (Keenan et al. 1974) and visual magnitude in the range 7.5 to 11.3 (Celis 1995). The spectral type is in the range M6e-M8 (Keenan et al. 1974).

Young (1995) has estimated the outflow velocity in T Ari to be 2.7 ± 0.7 km/s and the mass loss rate to be $0.6\pm 0.2\times 10^{-8} M_{\odot} \text{ yr}^{-1}$ from CO(3-2) observations. The IRAS $60\mu\text{m}$ images of a sample of circumstellar dust shell candidates have been fitted with a model of an unresolved central star surrounded by a dust envelope (Young et al. 1993). T Ari doesn't show any extended structure from their analysis.

The IRAS colors and LRS silicate feature strength at $10\mu\text{m}$ of T Ari have been fitted with a radiative transfer model by Hashimoto (1994) to obtain dust shell parameters. The reported values for the inner and outer dust shell radii were $100 R_*$ and $1000 R_*$ respectively; the dust temperature at the inner shell was 289 K. There is no evidence for the dust shell from our observations. SiO (Bujarrabal et al. 1987) and H_2O (Takaba et al. 1994) maser emissions have been detected in T Ari. However, there is no detection of OH emission (Lewis et al. 1995).

3.3. IRC−20445

The spectral type of IRC−20445 is M4 (Bidelman 1980). An alternative classification of M1 is given by Hansen & Blanco (1975). There is no positive detection of H_2O maser emission from this source (Deguchi et al. 1989, Dickinson et al. 1973).

This source was resolved earlier by a lunar occultation (Ridgway et al. 1977). Their derived angular diameter was 4 ± 1 mas, about a factor of two larger than our value listed in Table 4; correspondingly, also their estimate of the effec-

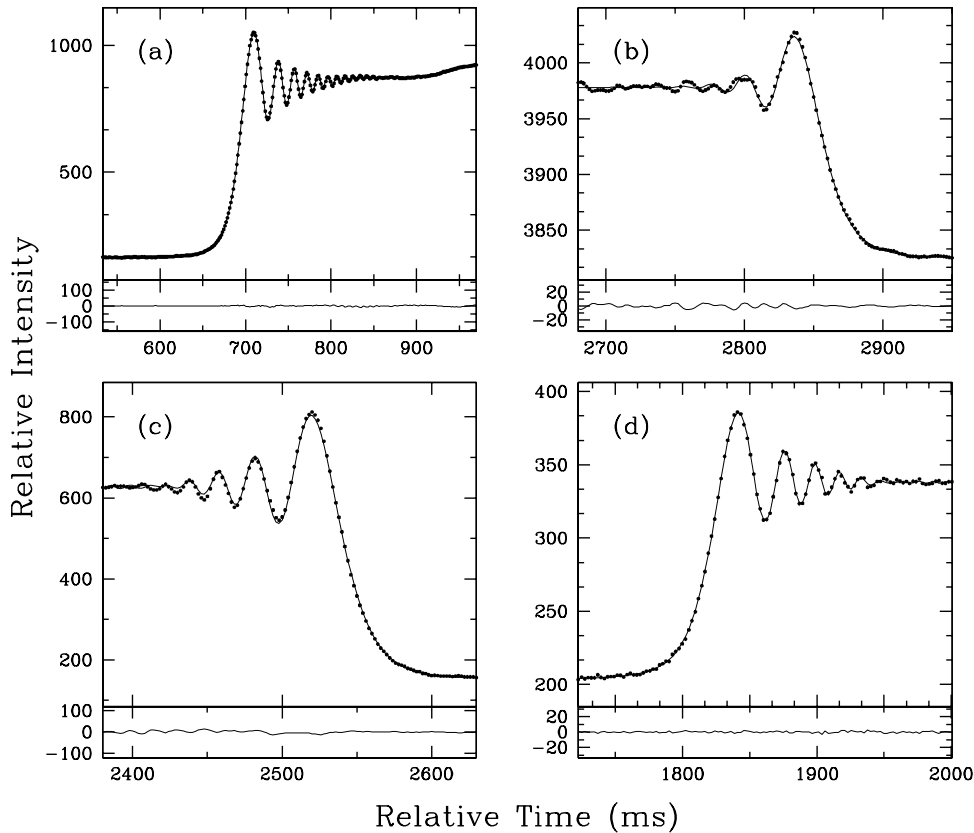


Fig. 1a–d. Examples of selected occultation lightcurves and our model fits to data are shown in the upper panels (dots and solid line respectively), while the residuals of the fits are shown in the lower panels with the same scale. From **a** to **d**, the stars are SW Gem, T Ari, IRC–20307 and IRC+20071.

tive temperature was remarkably low, 2520 ± 300 K. It is worth mentioning that the analysis of the lightcurve of this source by the authors above was not based on a least-squares analysis, but on visual inspection. However, this fact alone can not explain the discrepancy in the measured angular diameter. Ridgway et al. (1977) have also reported variability in this source of at least 0.3 magnitude at $2\mu\text{m}$. Given that a new occultation series of IRC–20445 will begin in mid-1999, it is worthwhile to reobserve this source and carry out photometric and spectroscopic monitoring to resolve this discrepancy.

3.4. IRC–20550

The occultation data of IRC–20550 were affected by scintillation. A polynomial of degree 5 with 3 free parameters has been used to model these effects.

The spectral type of IRC–20550 is G8 II-III (Keenan & McNeil 1989). Several LO events of this source were observed already in the previous series, all at visual wavelengths, namely by Evans & Edwards (1981), Radick et al. (1982) and Beavers et al. (1982). While these latter found the source to be unresolved at their resolution, Evans & Edwards (1981) derived a fully darkened disk angular diameter of 2.3 ± 0.4 mas. They also reported duplicity in this source. Radick et al. (1982) did not detect any duplicity from their observations, and derived a uniformly illuminated disk diameter of 1.27 ± 0.26 mas for the source. There is no detection of duplicity from our observation (Richichi et al. 1996a).

3.5. AB Gem

The angular diameter that we derive for this carbon star, listed in Table 4, when combined with the bolometric flux, implies a remarkably low effective temperature. Therefore, some discussion is necessary.

The spectrum of AB Gem was initially classified as a generic variable N type by Sanford (1944). A type of N3 was also reported (Grasdalen et al. 1983). We have obtained an IR spectrum at resolution $\lambda/\Delta\lambda \approx 1000$ at the TIRGO telescope in February 1996, covering the region of the K band around $2\mu\text{m}$. Although it is difficult to assign a spectral type from this spectrum due to the scarcity of good indicators, we have compared the slope of the continuum shortward of the onset of the CO band at $2.3\mu\text{m}$, with that of TU Gem. The result is that, apart from considerations of variability which could have some importance considering the 1.5 years elapsed between the recordings of the occultation and of the spectrum, AB Gem appears to be somewhat cooler than TU Gem, which is reported to have T_{eff} in the range 2400–2800 K (Ulla et al. 1997). This provides an indirect qualitative confirmation of our result listed in Table 4.

3.6. IRC+20071

The reappearance lightcurve of IRC+20071 is shown in Fig. 1d. A polynomial of degree 5 with 3 free parameters has been used to model the scintillation effect, which are already removed in the data shown in the figure.

Table 4. Angular diameter and effective temperature results

Source	ϕ (mas)	Bolom. flux (10^{-10} Wm^{-2})	T_{eff} (K)
SW Gem	2.80 ± 0.09	3.28 ± 1.38	3350 ± 380
AX Gem	3.02 ± 0.07	3.93 ± 1.92	3370 ± 440
IRC+20133	2.81 ± 0.09	6.63 ± 1.80	3985 ± 280
T Ari	7.08 ± 0.13	21.95 ± 7.03	3385 ± 280
IRC-20307	2.05 ± 0.16	1.56 ± 0.74	3315 ± 420
IRC-20445	1.74 ± 0.24	2.40 ± 0.99	3930 ± 510
IRC-20550	1.43 ± 0.15	3.85 ± 1.07	4880 ± 430
AB Gem	4.06 ± 0.09	1.43 ± 0.25	2330 ± 160
IRC+20071	2.71 ± 0.15	4.81 ± 1.32	3740 ± 280
IRC+10034	3.64 ± 0.07	5.89 ± 1.76	3400 ± 250
IRC+20141	2.11 ± 0.09	4.68 ± 1.41	4215 ± 340

IRC+20071 has been reported to be a LO binary with separation $0''.05$ (Dunham 1977). However, there is no positive detection of binarity from speckle interferometric observations in the optical at an angular resolution of $0''.03$ (Hartkopf & McAlister 1984). There is no evidence for a secondary component from our observations (Richichi et al. 1996b).

3.7. IRC+20141

Two events of IRC+20141 have been recorded at TIRGO. The second event was recorded under unfavorable observing conditions (close to full Moon and through clouds) and the data analysis could not reach any positive conclusion. However, we have resolved the source from the lightcurve of the first event. A polynomial of degree 5 with 2 free parameters has been used to account for the scintillation effect.

This source was observed earlier by Africano et al. (1978) at visual wavelengths, who reported duplicity in this source. However, there is no evidence for duplicity from our observation carried out at $2.2\mu\text{m}$ (Richichi et al. 1996b).

3.8. Bolometric fluxes and effective temperatures

From the angular diameter, the effective temperature T_{eff} can be directly derived, given the bolometric flux F . To compute this latter, we have fitted the photometric data of each of the sources in our sample. The data available from the literature have been used, complemented by our own photometry as listed in Table 3. In the case of IRC+20141 and IRC+20071 we assumed J, L & M magnitudes from the standard Johnson (1966) colors in the absence of any measurements, to constrain our fit.

The fits to the photometric data have been computed using a model with a black body. Interstellar extinction has been estimated on the basis of the presumed distance to the star, and accounted for. In those cases where infrared excess is evident, a second blackbody arising for the dust emission has been incorporated, as well as the additional circumstellar absorption. This was the case for six sources, namely SW Gem, AX Gem, T Ari, AB Gem, IRC-20307 and IRC-20445. However, the

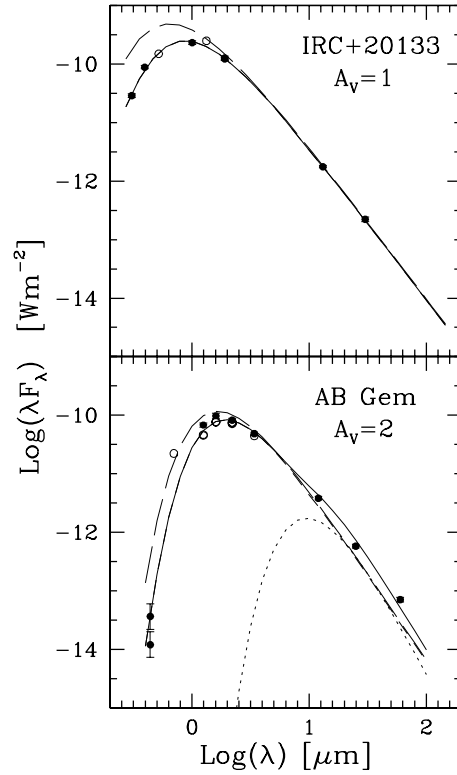


Fig. 2. Examples of black-body fits to photometric data. The two cases are discussed in the text.

shell contribution to the observed flux at $2.2\mu\text{m}$ is computed to be negligible in all cases. This explains why no evidence of dust shells is apparent from the analysis of our LO data.

In Fig. 2 we show two representative examples of our fits to the photometric data. A case representative of a single black body is that of IRC+20133, for which the fit required some amount of extinction, which however could not be uniquely constrained by the available data; the value $A_V=1.0$ is derived by minimizing the χ^2 and is consistent with the observed B-V color. In the case of AB Gem, we used two black bodies to fit the stellar component and the IR excess (the dashed and the dotted lines respectively in the lower panel of Fig. 2). In addition, we had to introduce an amount of extinction, which we estimate at $A_V=2.0$ on the basis of a minimization of the χ^2 of the fit. This incorporates both the extinction due to interstellar dust, and that caused by the circumstellar dust. The resulting total fit is shown as a solid line in the figure. In both panels of Fig. 2, the solid dots are the photometric data effectively used in the fit, while the open circles represent available data which were not used because the quality is not convincing, and are shown for reference only. This is the case for instance for the H band, where opacity is important.

The computed bolometric fluxes and the resulting effective temperatures are listed in Table 4. It can be seen that the relative errors are comparatively large: even considering that $\Delta T_{\text{eff}} \propto \frac{1}{4}\Delta F + \frac{1}{2}\Delta\phi$, the uncertainties in the bolometric flux account for the bigger part of the errors in the effective temperature.

This is due to different factors. Firstly, the sources in our sample lack a satisfactory photometric coverage in the literature, both in wavelength and in time. One should consider that late-type stars emit most of their energy in the near-IR, where unfortunately measurements are less frequently provided in the general catalogs. Reversely, the measurements in the visible region are sometimes not sufficient, because of the appreciable level of photometric variations exhibited by many of our stars at the shorter wavelengths. Secondly, extinction caused both by interstellar dust and by the circumstellar environment has a significant effect for many of the stars in our sample. This has been fitted as an additional parameter in our program, and the uncertainty is reflected in the final error. A program of near-IR photometry is under way at the TIRGO and Calar Alto observatories, with the purpose of ameliorating the situation described above.

The effective temperatures listed in Table 4 fit well the existing empirical calibrations quoted in Sect. 1. However, we postpone a thorough discussion of this comparison to another paper, which we will devote to the subject of a new calibration of the effective temperature of cool giant stars obtained from all the LO data collected during our long-term observational program. For this reason, we do not deal at this point with the necessary correction for limb darkening (which is typically a 2-5% effect on the angular diameter at near-IR wavelengths), and all the diameters listed in Table 4 are computed under the assumption of a uniform disk.

4. Conclusions

Lunar occultation observations of eleven cool giants in the spectral range K0 to M6 (including one carbon star) are presented in this paper. The quality of the lightcurves are good enough to resolve these giants from our observations. Nine giants are resolved for the first time from our observations. The measured (uniform disk) angular diameters fall in the range 1.43 to 7.08 mas with an average accuracy of 0.12 mas. Excluding the events of IRC–20307, IRC–20445 and IRC–20550, our measurements resulted in angular diameters with an accuracy better than 6%. These measurements have the potential to provide a valuable set of effective temperatures for cool giants with an accuracy < 3 % when bolometric fluxes for these giants become available with an accuracy < 10 %.

In this respect, it is interesting to compare the performance of the LO method against the current standards of long baseline interferometry. For this, we use the work of Perrin et al. (1997), which used the IOTA interferometer with baselines up to 21 m. Equipped with the FLUOR beam combiner, this provides currently the most accurate visibilities in the near-IR. The authors above have resolved nine stars in the range 10.0 to 20.2 mas, with an average accuracy of 0.18 mas. They use them to derive effective temperatures with a typical error < 100 K. The effective temperatures that we derive are consistent with the presently available effective temperature calibrations of late-type giants, but the errors are typically quite large due to the less than satisfactory knowledge of the bolometric fluxes. A program of

photometric observations to improve this situation is underway, and a detailed work on effective temperature calibration based on a homogeneous set of LO observations by our group will be published elsewhere.

Three sources from our sample, namely IRC–20550, IRC+20141 and IRC+20071, are reported to be LO binaries. However, we do not detect any binarity in these giants from our observations. We find evidence for circumstellar dust shell around six giants, namely SW Gem, AX Gem, T Ari, AB Gem, IRC–20307 and IRC–20445, from their infrared excess. However, we do not detect these dust shells from our observations as their contribution to the observed flux at $2.2\mu\text{m}$ is well below the detection limits. Our derived angular diameter of IRC–20445 is inconsistent with the earlier measurement by Ridgway et al. (1977). Future high angular resolution observations and photometric (and spectroscopic) monitoring of this source could resolve the discrepancy in the measured angular diameter.

Acknowledgements. This research has made use of the *Simbad* database, operated at CDS, Strasbourg (France). We thank G. Perrin for providing us with a copy of his work prior to publication. A.R. has been partially supported in his work by a Chretien Grant awarded by the American Astronomical Society.

References

- Africano J.L., Evans D.S., Fekel F.C., Smith B.W., Morgan C.A., 1978, *AJ* 83, 1100
- Beavers W.I., Cadmus R.R., Eitter J.J. 1982, *AJ* 87, 818
- Bidelman W.P. 1980, *Publ. Warner Swasey Obs.* 2, No. 6
- Bujarrabal V., Planesas P., del Romero A. 1987, *A&A* 175, 164
- Celis S.L. 1995, *ApJS* 98, 701
- Chengalur J.N., Lewis B.M., Eder J., Terzian Y. 1993, *ApJS* 89, 189
- Deguchi S., Nakada Y., Forster J.R. 1989, *MNRAS* 239, 825
- Dickinson D.F., Bechis K.P., Barrett A.H. 1973, *ApJ* 180, 831
- Dickinson D.F. 1976, *ApJS* 30, 259
- Dunham D.W. 1977, *Occ. Newsletter* 1, 120
- Dyck H.M., Benson J.A., van Belle G.T., Ridgway S.T. 1996, *AJ* 111, 1705
- Evans D.S., Edwards D.A. 1981, *AJ* 86, 1277
- Gennari S., Vanzi L. 1994 in *Infrared Astronomy with Arrays*, McLean I. (ed.), 351
- Grasdalen G.L., Gehrz R.D., Hackwell J.A., Casterlaz M., Gullizson C. 1983, *ApJS* 53, 413
- Hansen O.L., Blanco V.M. 1975, *AJ* 80, 1011
- Hartkopf W.I., McAlister H.A. 1984, *PASP* 96, 105
- Hashimoto O., 1994, *A&AS* 107, 445
- Johnson H.L. 1966, *ARA&A* 4, 193
- Keenan P.C., Garrison R.F., Deutsch A.J. 1974, *ApJS* 28, 271
- Keenan P.C., McNeil R.C. 1989, *ApJS* 71, 245
- Kukarkin B.V., Parenago P.P., Efremov Yu. I., Kholopov P.N. 1958, *General Catalogue of Variable Stars* (Moscow: Academy of Science, USSR Press)
- Lewis B.M. 1992, *ApJ* 396, 251
- Lewis B.M., David P., Le Squeren A.M. 1995, *A&AS* 111, 237
- Olson F.M., Raimond E., Neugebauer G. et al. (IRAS Science Team) 1986, *A&AS* 65, 607
- Nather R.F., McCants N.M. 1970, *AJ* 75, 963

- Perrin G., Coudé du Foresto V., Ridgway S.T., et al. 1997, A&A in press
- Radick R.R., Africano J.L., Rogers W.F., Schneeberger T.J., Tyson E.T. 1982, AJ 87, 885
- Ragland S., Chandrasekhar T., Ashok N.M. 1997, MNRAS 287, 681
- Richichi 1997, IAU Symposium 189, Bedding T., Booth A.J., Davis J. (eds.), p. 45
- Richichi A., Lisi F., Di Giacomo A. 1992a, A&A 254, 149
- Richichi A., Di Giacomo A., Lisi F., Calamai G. 1992b, A&A 265, 535
- Richichi A., Chandrasekhar T., Lisi F., et al. 1995, A&A 301, 489
- Richichi A., Calamai G., Leinert Ch., et al. 1996a, A&A 309, 163
- Richichi A., Calamai G., Leinert Ch., Stecklum B. 1996b, A&A 322, 202
- Ridgway S.T., Wells D.C., Joyce R.R. 1977, AJ 82, 414
- Sanford R.F. 1944, ApJ 99, 145
- Takaba H., Ukita N., Miyaji T., Miyoshi M. 1994, PASJ 46, 629
- Ulla A., Thejll P., Kipper T., Jørgensen U.G. 1997, A&A 319, 244
- White N.M., Feierman B.H. 1987, AJ 94,751
- Young K. 1995, ApJ 445, 872
- Young K., Phillips T.G., Knapp G.R. 1993, ApJS 86, 517